Functionalization of SBA-15 by an Acid-Catalyzed Approach. A Surface Characterization Study

Nuria García,[a] Esperanza Benito,[a] Julio Guzmán,[a] Pilar Tiemblo,[a] Victoria Morales,[b] and Rafael A. García[b]

[a] Instituto de Ciencia y Tecnología de Polímeros (CSIC). Juan de la Cierva, 3. 28006 Madrid, Spain.

[b] GIQA. Departamento de Tecnología Química y Ambiental. ESCET. Universidad Rey Juan Carlos. 28933 Móstoles (Madrid), Spain.

Published on: microporous and mesoporous materials 106 (2007) 129-139

doi:10.1016/j.micromeso.2010.01.010

Abstract

The functionalization of a mesoporous ordered silica, SBA-15, by a grafting strategy has been successfully achieved. The derivatized SBA-15 products with trimethylmethoxy silane, vinyltrimethoxy silane and octyltrimethoxy silane have been characterized by BET analysis, DRX analysis, thermogravimetric analysis and NMR techniques. The use of p-toluenesulfonic acid as catalyst and the azeotropic distillation of the alcohol generated in the hydrolysis and condensation of the silanes allowed the incorporation of high amounts of organic loading in shorter times as compared to conventional toluene reflux method. The surface of the resulting materials has been thoroughly analyzed and the concentration of total and residual silanols and silane molecules attached on the surface has been quantitatively determined. Being the as-modified SBA-15 materials hydrophobic as a rule, the accessibility of the residual silanol population, evaluated by a deuterium exchange method and subsequent cross polarization NMR analysis, depends on the nature of the surface organic layer.

Keywords: Mesopororous material; SBA-15; Hybrids; Organosilanes; Hydrophobic Character; deuterium exchange

1. Introduction

Since the development of the M41S mesoporous materials family in 1992 by the Mobil Company [1], the number of studies on synthesis modifications to obtain new related materials has exponentially grown. In this regard, the so-called SBA silica mesoporous family, synthesized by Stucky and co-workers [2,3], offers new perspectives on this interesting field. SBA-15, a two-dimensional hexagonal mesostructured silica, is one of the most remarkable materials of this family due mainly to its high surface area, large pore size (> 6 nm), narrow pore size distribution and high

thermal stability. These distinct features make SBA-15 desirable in a wide variety of research areas for many different applications, shape-selective heterogeneous catalysis, adsorption, separation, sensing, ion exchange, chromatography, controlled immobilization or release of biologically active molecules or use as nanoreactors among others [4-10].

A major drawback of these materials lies on their relatively inert nature towards organic transformations, so, previous to their applicability, the surface modification is a usual requirement [11]. Moreover, the controlled organic modification allows custom-tailoring surface chemical and physical properties, broadening thereby the use of the mesoporous materials in more specific applications.

The most widely used strategies to modify the surface and then obtain organo-inorganic hybrid mesoporous silica materials are (i) the direct synthesis or co-condensation and (ii) the two-step post-synthesis grafting. The first method is based on the co-condensation of the siloxane and organosilane precursors in a one-pot synthetic approach. The siloxane precursors determine the structure, while the organosilanes contribute both to build the structure and to functionalize the material surface. The resulting product incorporates a special homogenous distribution of organic groups [12-16]. However, the main shortcomings associated to this method are the loss of the structural order regarding its pure siliceous counterparts, the need to adequately choose the suitable organosilanes and siloxanes to avoid phase separation and Si-C bond cleavage, and the defect sites created during the synthesis and the template removal. In addition, the use of low-temperature processes, such as solvent extraction, to preserve the organic functional groups on the mesoporous silica induces a decrease in the hydrothermal stability of the final material. Co-condensation generally requires also the

use of large volumes of organic solvents and, therefore, the process can become uneconomical and environmentally unfriendly.

On the other hand, the incorporation of organic moities by the post-synthesis method consists of the modification of the internal mesostructured silica surface by the subsequent reaction of the free silanols with organosilanes [17]. Grafting presents some interesting advantages arising from (i) the ordered resulting material after the process, (ii) the great variety of functional groups which can be chosen depending on the application, and in this sense, literature shows a wide spectrum of organo-tethered mesoporous materials with several reactive and non-reactive functionalities [18-20], and (iii) the as-obtained materials display a higher hydrothermal stability.

The usual reaction conditions for the post-synthesis method are a 24-hour reflux in a non-polar solvent (commonly toluene) in the presence of an excess of the organosilane to be anchored onto the internal surface by the reaction with the geminal and single SiOH groups. Therefore, the amount of organic loading incorporation is closely related to the initial density of surface silanol groups. From this point of view, the study of the surface chemistry of the mesoporous material, before and after derivatization, is crucial in order to evaluate the degree of modification.

Independently on the synthetic approach employed to functionalize the material, the most difficult task in dealing with organophilized silicas is an unambiguous characterization of the surface nature. ^{29}Si and ^{13}C nuclear magnetic resonance experiments (^{29}Si and ^{13}C NMR) have been extensively probed to be an excellent method for the study of silica surfaces [20-28]. Magic angle spinning (MAS) ^{29}Si NMR spectra with and without cross polarization (CP) allows a quantitative evaluation of the different silicon sites populations present in the organophilized materials, i.e. those of bare silica, Q^2, Q^3, and Q^4 sites, and those of the trifunctional and monofunctional

organosilanes, T^n and M, respectively. Following standard notation, the superscript stands for the number of Si-O-Si bonds, thus, Q^2 refers to geminal silanols and Q^3 to single ones.

In what follows, the results obtained by applying a simple and effective post-synthesis approach to functionalize a mesoporous SBA-15 will be presented. The grafting reactions have been carried out in the presence of an acid catalyst, p-toluenesulfonic. The yield in the incorporation of the organic groups is higher and the reaction time shorter than in the previously described conventional method. Furthermore, the grafting reaction proceeds in a controlled manner, remaining the mesoporous character of the material unaffected.

To explore the possibilities of the post-synthesis approach, different organosilanes have been tested. Mono- and trialkoxysilanes with short and long alkyl chains, vinyltrimethoxy, octyltrimethoxy and trimethylmethoxy silanes, have been successfully grafted on the SBA-15 inner surface. The use of organosilanes with functionalizable organic groups gives the resulting materials many favorable features to broaden the application fields. In this regard, vinyl functionalities exhibit ample reactivity and display versatile precursor moieties for both subsequent organic transformations and metal incorporation reactions. Thus, the introduction of such reactive groups on the SBA-15 keeping a sufficiently large pore volume, makes the material very interesting for catalytic and sensing applications [29,30].

On the other hand, as an example, the hydrophobization of mesoporous silicas with trimethylsilyl groups has been found to retard the drug release in biomedical applications [31]. On its own, the coating with bulky and non-reactive large alkyl chains, such as octyl, is a usual derivatization reaction when dealing with chromatographic phases.

In addition, to calculate the amount of silanol groups before and after derivatization reactions, the surface structure of the materials has been thoroughly studied by means of ^{29}Si and ^{13}C NMR. The textural properties and the thermal stability of the organic coverage have been also determined. Finally, the accessibility of the residual silanol populations have been qualitatively analyzed using a deuterium exchange method and subsequent ^{29}Si CP NMR analysis of the deuterated samples.

2. Experimental section

2.1. Chemicals

PEO-PPO-PEO triblock copolymer (Pluronic P123), tetraethyl orthosilicate (TEOS, 98%), deuterium oxide (D_2O, 99.9% atom %D) and acetonitrile anhydrous (99.9%) were purchased from Aldrich, and used as received. Hydrochloric acid 35 % extra pure was supplied by Scharlau. The alkoxysilanes: octyltrimethoxy (Lancaster, 90 %), vinyltrimethoxy (Aldrich, 97 %), and trimethylmethoxy (Aldrich, 99 %) were used without previous purification. The p-toluenesulfonic acid (PTSA, Aldrich, 98.5 %) was also used as received.

2.2. Synthesis of pure-silica SBA-15

Pure silica SBA-15 material was prepared following the method described by Zhao et al. [3]. In a typical synthesis 4 g of block copolymer surfactant Pluronic 123 was dissolved at room temperature under stirring in 125 ml of 1.9 M HCl. The solution was heated up to 40 ºC. Then, 8.58 g of TEOS was added to the solution and stirred for 20 h. The mixture was aged at 100 ºC for 24 h under static conditions. The solid was filtered off, washed with deionized water and dried at room temperature overnight. Calcination for template removal was conducted in air atmosphere at 550 ºC for 5h.

2.3. Synthesis of organic-functionalized SBA-15

The alkoxysilanes used for the reactions are listed in Table 1.

Insert Table 1

The resulting materials are named according to the assigned nomenclature in this table. A detailed description of the reaction procedure is as follows, 1 gr of as-synthesized SBA-15 (water content around 4% as determined by TGA) and 150 mL of toluene were placed in a three-necked flask equipped with a mechanical agitator and a Dean-Stark reflux condenser. The mixture was stirred at 50 ºC during 30 minutes to achieve a homogeneous dispersion; after that, 0.007 gr of PTSA and 2 mmoles of the alkoxysilane were added. In the synthesis of TMS-3, three-fold quantities for catalyst and alkoxysilane were used. For the synthesis of sample VTS-w no PTSA was added. The mixture was heated up to reflux temperature and kept stirring at this temperature during 2 hours. The reflux time for the sample TMS-2 was 7 hours. After cooling, the products were isolated from the reaction medium by centrifugation and purified by means of repetitive washing in ethanol (three times) and further centrifugation. Finally, prior to analysis, the reagent-free materials were dried at 100 ºC for 12 hours.

The sample VTS-TMS was obtained from the previously synthesized VTS after a second derivatized reaction with trimethylmethoxy silane under the above described reaction conditions. The same procedure was applied for the synthesis of OTS-VTS from OTS and a second derivatization with vinyltrimethoxy silane.

2.4. Deuterium exchange method

In order to obtain information on the accessibility of residual silanol populations, deuterium exchange in acetonitrile and D_2O experiments were performed. The deuterium exchange was performed according to a procedure described by Scholten et al. [25]. Typically, 0.3 g of organically modified SBA-15 material were placed in a 100 mL flask under nitrogen atmosphere and 10 mL acetonitrile were added while stirring.

The suspension was treated in ultrasonic to avoid pore-filling gases before 1 mL of D2O addition. After 15 minutes stirring, the solvent was evaporated under reduced pressure. The procedure was thrice repeated for each sample. Subsequently, the solids were dried under vacuum overnight and kept under nitrogen. Every step was performed under nitrogen atmosphere to prevent air interaction during the deuterium exchange.

2.5. Characterization

The thermogravimetric analysis, TGA, was undertaken in a TA Q-500 at a heating rate of 10 ºC·min^{-1} and a nitrogen flow of 60 mL·min^{-1}.

Carbon content in the derivatized products was obtained by a LECO CHNS-932. Data on carbon content for the different samples are compiled in Table 1.

Mesoscopic ordering of silylated materials was checked by X-ray diffraction patterns recorder on a PHILLIPS X'PERT diffractometer using the CuKα radiation. Typically, the diffractograms were collected in the range from 0.6º to 5.0º (2θ) for mesostructured materials with a resolution of 0.02º and a counting time of 10 s.

The textural properties of raw SBA-15 and the derivatized materials were characterized by using nitrogen adsorption-desorption isotherms at 77 K. The measurements were conducted on a MICROMERITICS TRISTAR 3000 instrument. Previously, the samples were outgassed at 200 ºC for 4h under nitrogen flow. The surface area measurements were performed according to the B.E.T method from the nitrogen adsorption points in the range P/P_0 = 0.05-0.2. Pore size distribution was determined applying the Barrett-Joyner-Halenda model (B.J.H) applied to the adsorption branch of the isotherm, assuming cylindrical pore geometry. For each sample the average pore size was estimated as the diameter corresponding to the maximum of the pore size distribution curve. Total pore volume was taken at a relative pressure P/P_0 of 0.985. The micropore volume was determined by the t-plot method in the selected

range of the adsorption branch of the isotherm. The as-determined textural properties: BET surface, S_{BET}, pore size, d_A, total pore volume, V, and micropore volume, V_{micro}, are gathered in Table 1.

To confirm the hexagonally arranged uniform pore structure of the different modified samples, transmission electron micrographs were collected on a Phillips TECNAI 20 microscope equipped with a LaB6 filament under an accelerating voltage of 200 kV. Prior to the observation, the samples were dispersed in acetone, stirred in an ultrasonic bath and finally deposited over a carbon-coated copper grid.

Solid-state ^{13}C and ^{29}Si MAS NMR experiments were performed on a Varian Infinity 400 spectrometer with a 9.4 T magnetic field. These nuclei resonate at 100.53 and 79.41 MHz respectively, H/X 7.5 mm MAS probe and ZrO_2 rotors spinning at 6 kHz were used. On CP experiments, the cross polarization time was determined to guarantee the total proton polarization verifying the Hartmann-Hann condition. In addition, to allow an accurate quantification of silanol groups, ^{29}Si NMR spectra using one pulse sequence were also obtained. For ^{13}C acquisition, $\pi/2$ pulse, number of scans, repetition delay and contact time were, 4.25 μs, 2000 sc, 3 s and 1 ms. The ^{29}Si experiments were performed after 3000 scans, $\pi/2$ pulse of 3,5 μs and 15 s of repetition time. On ^{29}Si CP experiment contact period was 10 ms. As cross polarization depends upon heteronuclear dipolar interaction, the greater distance from silicon to protons is manifested in a larger cross polarization time constant. Both ^{13}C and ^{29}Si chemical shifts were externally referenced to adamantane and tetramethylsilane, respectively. The deuterium-exchanged samples were loaded into rotors that had been rinsed with 99.9% D_2O. All sample transfers took place under a dry nitrogen atmosphere in a glove box.

3. Results and discussion

3.1. Special features derived from the reaction conditions

The identity label of the organic modification reactions carried out in this work is the catalysis by PTSA and the Dean-Stark azeotropic distillation of the alcohol produced in the hydrolysis of the reagent. To the best of our knowledge, there is no previous reference to the use of these conditions for organic modification of mesoporous silicas. Engelhardt and Mathes [32] mentioned that the rate of the organically derivatization of non porous silica for chromatography phases was improved by removing the alcohol produced in the hydrolysis and by the addition of such a catalyst, however, they neither explain the effects nor show comparative results. The effects of this acid on the reaction are, on the one hand, a rapid rate of incorporation, since two hours is almost enough to reach a plateau in the carbon content (see %C for TMS-1 and TMS-2 in Table 1), and on the other hand, a higher amount of organic loading than in the absence of the catalyst, as can be deduced by comparing the carbon content in the samples VTS and VTS-w (similar results were found in the products of reactions with other silanes in the presence and absence of catalyst). In this regard, although the difference in carbon content between both samples could seem not pronounced, the ^{13}C CP NMR spectra in Fig. 1 will help to explain the effects of PTSA on the reaction.

Insert Figure 1

The ^{13}C NMR spectrum of sample VTS-w (Fig. 1a) shows mostly the signals assigned to alkoxy groups, located at δ=59, 16 (ethoxy) and 49 ppm (methoxy) [22,23], whereas, the bands at δ =128 and 136 ppm, corresponding to vinyl groups, are predominant in the ^{13}C NMR VTS spectrum (Fig. 1b). Therefore, the addition of PTSA clearly enhances the hydrolysis of the silanes. A quantitative analysis of the ^{13}C NMR signals reveals that in the case of VTS, the 88% of the carbon nuclei present in the

sample spectra are vinyl groups, being less than 40% in the VTS-w sample. This means that, according to the carbon contents listed in Table 1, the incorporation of silane molecules is increased by more than three with the presence of the catalyst. It should be noted that the ethoxy groups present in the samples must come from the chemical or physical sorption of ethanol during the drying treatment after washing. Based on the fact that the ^{13}C NMR spectra of samples TMS-1 and TMS-2 did not show any signals assigned either to methoxy or ethoxy groups, the chemical reaction of the generated methanol or the washing ethanol with SBA-15 surface silanols and the physical sorption of ethanol in the organically modified samples were discarded. The presence of these signals in VTS and VTS-TMS must be thereby attributed to the reaction of ethanol with hydrolyzed OH groups from the grafted species (also more accessible than those on the surface). On the contrary, the low organic load in the VTS-w sample makes the surface SBA-15 silanols fully accessible to the ethanol sorption and, in this case, ethoxy groups might be grafted directly on the surface.

On the other hand, comparing the ^{13}C NMR spectra of VTS and VTS-TMS (Fig. 1c), the following features must be pointed out: (i) the presence of the signal at δ=0 ppm assigned to the trimethyl silane molecules, (ii) the signals in VTS-TMS corresponding to alkoxy groups are quantitatively very similar to those in the VTS spectrum, and (iii) the vinyl group signals in the VTS-TMS spectrum are less resolved than in the VTS one, which denotes a close spatial interaction of the vinyl groups with the trimethyl silane moieties.

The effects of PTSA on both the hydrolysis and incorporation of silane molecules will modify the structure of the organic layer grafted on the surface; a quantitative and qualitative analysis of this will be the matter of study in the following sections.

Previously, the success in the grafting of the organic groups on the SBA-15 silica surface has to be assessed. Thus, Table 1 shows the results from N_2 adsorption-desorption isotherms at 77 K. Surface area, total pore volume and pore diameter of the modified samples are lower than the corresponding values for the parent SBA-15 as a consequence of the organic coverage. The decrease in the pore volume also assesses that lining is happening inside the mesopore.

Insert Figure 2

Fig. 2 shows the isotherms for samples with different amount of organic loading. All of them exhibit type IV isotherms, featuring a sharp increase due to capillary condensation at relative pressure P/P_0=0.5-0.7 characteristic of mesoporous materials with a uniform pore size distribution. This result reveals that the mesoporous nature of the material is preserved even though the grafting has occurred. Moreover, the existence of micropore volume (Table 1) in all the samples, although diminished compared to the raw material, confirms that the structure is preserved and scarce pore blocking effects take place.

The evidence that the mesoporous structure is maintained after the grafting reactions is also supplied by XRD analysis. The organically modified samples show XRD patterns similar to that of the parent SBA-15, exhibiting a strong [100] reflection peak characteristic of the mesoporous material, as one can expect considering that the incorporation of organic chains should not affect the original structure. Besides, the organically modified samples showed no peak position shift to high or low angle region, indicating that after the post-synthesis treatment no depolymerization or condensation of the silica wall occurs.

The mesoporous character of the modified samples was definitely confirmed by Transmission Electron Microscopy (TEM). A TEM image of the VTS-TMS sample

showing the honey-comb like structure typical of an hexagonal array with highly regular parallel layers is supplied as supplementary data (Fig. 1S).

Thermogravimetric analysis has been used to evaluate the organic coverage decomposition temperature. In Fig. 2S (supplementary data) the thermogravimetric curves of some selected samples are depicted. The onset of thermal degradation is over 200 ºC and very similar for the organically modified samples. This is another evidence of the grafted nature of the organic coverage.

The weight loss estimated by TGA is in agreement with the carbon content in the samples. However, the TGA data on their own could lead to an erroneous estimation of the organic mass incorporation. See, as an example, the TGA curves of VTS and VTS-TMS samples showing almost the same weight loss, though, as described before, they differ significantly in both the amount and nature of the grafted silanes.

The reaction conditions employed have allowed then to obtain highly loaded, thermally stable organically modified SBA-15s preserving however their mesoporous nature.

3.2. Chemical structure of the surface: ^{29}Si NMR experiments

The characterization of the chemical structure of the surface of organically modified silicas is a must, since the surface nature is going to determine the properties and, therefore, the applicability of the material. For this purpose, the ^{29}Si NMR is a powerful technique. By means of NMR experiments, the structure of the organic surface coverage, the number of initial and residual silanols on the surface and the accessibility of the latter can be evaluated. In what follows, the elucidation of the chemical structure by using this technique will be described.

The ^{29}Si CP NMR technique, which enhances the sensibility of the silicon atoms near to protons, enables a thorough characterization of the surface species. The CP

NMR experiments have been widely used to quantitatively estimate the SiOH groups on solid surfaces [22-25]. However, to assure a reliable quantitative determination, CP relaxation dynamics must be previously examined. Therefore, obtaining quantitative information from CP spectra requires the deconvolution of Q spectral region into the bands Q^4, Q^3, and Q^2 (at $\delta \approx -112$, -102, and -92 ppm, respectively) [21] of measurements obtained varying the contact time in CP experiments. In this work, we have preferred to limit the deconvolution process, and, therefore, the quantitative analysis, to the ^{29}Si NMR spectra without CP. Nevertheless, the CP NMR spectra provide valuable qualitative information on the spectral features, such as the number, the intensity, the width and the position of the signals, which will help to perform a deconvolution fit based on realistic criteria.

Insert Figure 3

Fig. 3 shows the ^{29}Si CP NMR spectra of the pure SBA-15 (Fig. 3a) and some modified samples. In these spectra, the grafted nature of the organic molecules is confirmed by the presence of the T^i signals assigned to mono (T^1)-, di (T^2)-, and tri (T^3)-fold Si-O linked silicons at $\delta \approx -64$ ppm, $\delta \approx -73$ ppm, and $\delta \approx -81$ ppm, respectively in the case of VTS-TMS (Fig. 3d) and VTS-w (Fig. 3b), and the M signal assigned to $(CH_3)_3$Si-O molecules in the TMS-3 (Fig. 3c) and the VTS-TMS (Fig. 3d) spectra. The intensity of T^i and M signals in the TMS-3 and VTS-TMS spectra is very strong denoting a high organic loading. It is worth remarking that, as expected, not only the intensity of the T region in the VTS-TMS spectrum is higher than in the VTS-w spectrum but also the distribution of the signals is very different. The signals of T^2 and T^3 are the main components in the VTS-TMS, being the T^1 almost non-existent. This event is usually associated to the formation of a crosslinked organic layer on the surface [23,33], and is consistent with the low concentration of non-hydrolyzed alkoxy units

observed in the ^{13}C NMR spectrum (Fig. 1c). On the contrary, although the T signals are less intense in the VTS-w, the predominant character of T^1 and T^2 and the lack of T^3 can be suspected. Another interesting feature is the decrease in the Q^3 signal on going from the spectrum a to d in Fig. 3, indicating that the largest extent of the surface reaction occurs in the VTS-TMS sample. Nevertheless, even in this case, the shape of the Q region suggests an important contribution of Q^3 signal, what implies a high concentration of residual silanols. In addition, the existence of geminal silanols can be assessed in all modified samples. The knowledge of these CP NMR spectral features has enabled a realistic deconvolution of the signal envelope, and hence, allowed a quantitative determination of the ^{29}Si NMR signals, which is shown in the next section.

3.2.1. A quantitative determination of the initial and residual geminal and single silanols.

Fig. 4 shows the ^{29}Si NMR spectra of the raw SBA-15 (Fig. 4a) and some of the organically modified samples. To achieve a quantitative determination of the residual silanols on the surface, the deconvolution of the signals in the spectra has been carried out (some examples of the fits are showed in Fig. 3S of Supplementary Data). The use of three Gaussians for the Q^i sites adequately reproduces the spectral signals as occurs with other types of silica [22,24,25]. The variation in peak widths within the samples was not pronounced, being the average values 477 Hz for Q^2, 486 Hz for Q^3, and 756 Hz for Q^4 in good agreement with literature data [24]. The estimated error in the determination of the deconvoluted areas was found to be less than 10%.

Insert Figure 4

The molar fractions of the Q^i, T^i and M species were determined from the areas of the signals after the decomposition fitting. Subsequently, the molecular weights of the samples were calculated as a sum of the products of molecular weights by molar

fractions for each species in the sample, considering as the molecular weights for Q^4, Q^3, Q^2, and M species, that of molecules $Si(O_{0.5})_4$, $Si(O_{0.5})_3OH$, $Si(O_{0.5})_2(OH)_2$, $Si(CH_3)_3$ respectively [20]. The molecular weights for the T^i species were estimated by making use of the information on alkoxy groups provided by the ^{13}C NMR spectra and the relative abundance of each T^i species in every sample. The loss of one hydrogen atom in the surface reaction has been also taken into account for the estimation of the molecular weight of the samples. Once the molecular weight of the sample was known, the residual unreacted geminal and single silanol concentrations were calculated by dividing the molar fractions of Q^2 and Q^3, respectively, by this total molecular weight. The number of residual silanols per surface unit (OH^{res} in nm^{-2}) was obtained using the S_{BET} value of the raw SBA-15 (Table 1).

Insert Table 2

Table 2 compiles the results on the molecular weight, molar fractions of Q^i species and the total number of residual unreacted silanols for some samples. It goes without saying that for SBA-15 the number of residual silanols represents the number of initial silanols in the raw material. A direct way to check the reliability of the quantitative analysis performed is to calculate the theoretical carbon content from the T^i and M species molar fractions and the sample molecular weight. The as-calculated carbon contents listed in the last column of Table 2 agree very well with those experimentally obtained collected in Table 1, except for OTS-VTS where the error in the estimation of the molecular weight is larger due to the coexistence of six different T^i species.

Before discussing in detail the results gathered in Table 2, an alternative method to estimate the initial number and the extent of the reaction on geminal and single silanols will be presented. From the peak areas determined after curve fitting and the

carbon content values, the initial number of surface silanols, OH^i, for the raw SBA-15 can be calculated using Equation (1) [23]:

$$OH^i = \frac{\Gamma(1 + f + f_g^r)}{f} \quad (1)$$

where Γ is the number of attached silane silicons per surface unit, *f* the ratio of attached silane silicons to residual silanols silicons, and f_g^r the fraction of geminal silanol sites in the modified sample. Γ was calculated from the carbon contents listed in Table 1 by the equation [34],

$$\Gamma = \frac{N_A \%C}{S_{BET}(1200 n_C - \%C(M-1))} 10^{-18} \quad (2)$$

where N_A is Avogadro´s number, n_C is the number of carbon atoms in the silane and *M* is its molecular weight. For samples modified with trifunctional silanes, the values of *M* and n_C were estimated as average values accounting for the molar fractions and molecular weights of T^i species in every sample. It must be noticed that for this calculus, the assumption of one single graft per trialkoxy silane was made. This means that tri- and bigrafting species were not considered. The former can be rejected based on literature [34], the latter is likely to exist but, unfortunately, difficult to quantify. In any case, the differences in Γ calculated assuming the existence of a fraction of bigrafted species can be considered not relevant.

On the other hand, the parameters *f* and f_g^r were obtained from the deconvoluted areas of the resonance signals in ^{29}Si NMR spectra for attached silane species (T^i and/or M), I_S, geminal silanols, I_g, and single silanols, I_l, as follows [23]: $f=I_S/(I_g+I_l)$, and $f_g^r = I_g/(I_g+I_l)$. In addition, knowing the value of f_g^i, which refers to the starting SBA-15 and was found to be 0.12, it is possible to calculate *the extent of the reaction, θ,* given as the

ratio of reacted silanols to initial silanols on the surface. On their turn, the relative reaction of the two distinct surface silanols, geminals and singles, can be referred to θ_g and θ_l, respectively. Algebraic manipulation of the above introduced parameters leads to the following relationships [23]:

$$\theta = \frac{f(1+f_g^i)}{1+f+f_g^r} \tag{3}$$

$$\theta_g = \frac{1+f-\frac{f_g^r}{f_g^i}}{1+f+f_g^r} \tag{4}$$

$$\theta_l = \frac{1}{1-f_g^i}\frac{f+f_g^r-f_g^i}{1+f+f_g^r} \tag{5}$$

The OH^i, Γ, θ, θ_g, and θ_l as-calculated values for the samples TMS-2, TMS-3, VTS, and VTS-TMS are listed in Table 3. The OTS-VTS sample was not analyzed in this way because the uncertainty for the molecular weight estimation would lead to erroneous results.

Insert Table 3

From the observation of Fig. 4 and the results in Tables 2 and 3, many interesting conclusions can be drawn. Firstly, although the fraction of initial geminal silanols is apparently small (around 22%), it agrees well with literature data which report a fairly constant fraction of geminal silanols of 30 % in amorphous non porous silicas after temperature treatments [24]. Given that all the modified samples were obtained from the same batch of raw SBA-15, the OH^i values in the second column of Table 3 should be identical and fit with the OH^{res} for the SBA-15, namely 3.82 nm^{-2}. Within the experimental and fitting errors, it can be stated that these values agree well in the case of TMS-2 and TMS-3, and they are significantly lower for VTS and VTS-TMS. This lowering, around 20 % for the VTS sample, can be ascribed to the plausible

occurrence of bigrafted species, as mentioned above, which cannot exist in the case of the monoalkoxysilane. Supporting this hypothesis, it must be pointed out that the sum of Γ and OH^{res}, which obviously results in the number of initial silanols, is also lower for the samples VTS and VTS-TMS than for TMS-2 and TMS-3. Assuming 3.82 OH groups per nm^2 and that the error made in the estimation of Γ is not large, every three silanes attached to the surface in the VTS sample, one is bigrafted to the silica. This data is consistent with the higher extent of reacted geminal silanols, θ_g, for samples VTS and VTS-TMS compared to TMS-2 and TMS-3. Actually, all the modified samples show a lower conversion for the geminal silanols as compared to single ones. These results can be interpreted in terms of either the lower reactivity or/and the lower accessibility of geminal silanols. However, none of these hypotheses can be assured or demonstrated from the results of this work. What can be assessed is that the suspected spatial proximity between geminal and single silanols can give rise to steric constraints to the reaction of additional silane molecules on silanols close to already attached silane molecules. In the case of trifunctional molecules, their ability to bigraft and condense enables them to react with spatially close silanols, enhancing the conversion of both geminal and single silanols as occurs experimentally. Furthermore, steric hindrance in the incorporation of new molecules to the surface exists, what is clearly seen by the higher OH^{res} value for OTS-TMS compared to VTS or VTS-TMS. Being OTS also a trifunctional silane, the reaction of either geminal or single silanols close to a grafted silane and also probably the condensation between silane molecules will be hindered by the bulky octyl side group. Consequently, if a high extent of surface reaction is required, the use of small side-group trifunctional silanes is highly recommended.

On the other hand, the VTS and VTS-TMS spectra (Fig. 4e and 4f, respectively) shows that the end-capped reaction leads to the practical absence of T^1 species in the

latter sample. Given that the diminishing in Q^3 sites in VTS-TMS compared to VTS agrees well with the reaction of the monoalkoxysilane with single silanols, that the differences in Q^2 populations can be ascribed to fitting errors and that the non-hydrolyzed alkoxy groups are practically the same in both samples, the second derivatization reaction provides not only a higher extent of the surface reaction but also a further condensation of hydrolyzed OH groups coming from spatially close T^1 and T^2 species. This contributes to the formation of a crosslinked organic layer on the silica surface [23].

It is remarkable that even after the modification reaction there is a high concentration of residual unreacted silanols on the samples. Increasing the reaction time or the reagent stoichiometry did not lead to outstandingly improving the extent of the reaction. As mentioned above, a fraction of surface silanols must be too sterically hindered to be consumed in the reaction. Besides, the existence of silanols inside the pore walls, which can hence be considered inaccessible for any reaction, is well known [15]. The accessibility to reactive molecules or to water (hydrophobic character) of these remaining silanols is a crucial factor in many applications of mesoporous silicas. This issue has been evaluated by using a deuterium exchange method and the results are presented in the forthcoming section.

3.2.2. Accessibility of the residual silanol population.

A very intuitive test to explore the hydrophobic character of the modified sample is to check the water wettability. A picture showing some derivatized samples in water suspension after three days of immersion is presented in Fig. 5. This simple test provides valuable information. For example, the increase of the reaction extent from 0.28 in TMS-2 to 0.38 in TMS-3 induces a dramatic change in the wettability behavior, being the former partly hydrophilic and the latter non-wettable. In this regard, the end-

capped reaction in VTS-TMS as compared to VTS causes the same effect. The high wettability of VTS is basically explained by the presence of the hydrolyzed OH groups from the attached silane, since the number of OH^{res} is less than in TMS-3. The behavior of VTS-w in water is clearly different from the rest showing no hydrophobic floating layer due to the of an organic surface coverage. Concerning the OTS-VTS, the non-wettable character must be caused by the incorporation of long alkyl chains as the number OH^{res} is even higher than in the TMS-3 sample.

Insert Figure 5

For a better analysis on silanol accessibility, the deuterium exchange reaction of residual silanols has been carried out. Fig. 6 shows the ^{29}Si CP NMR spectra of SBA-15 and some organophilized samples before and after deuterium exchanging. The use of D_2O to chemically exchange accessible surface silanol protons for deuterons is a usual technique in chromatographic studies on silica surfaces [35]. The combination of this reaction and the analysis with CP NMR enables to study the silanols buried in the silica structure and the accessibility and shielding of the unreacted silanols on the surface [23,25]. It can be assumed that on the silica surface all silanols are deuterium exchangeable, leaving only internal silanols buried into the silica walls to be detected by CP NMR. It has been also demonstrated that, in contact with a good solvent for alkyl chains, any residual unreacted silanol on an alkylsilylated silica surface will be accessible to a D_2O exchange. This is so because of motions in the grafted alkylsilane layer, which will create holes that allow the access to D_2O molecule [36]. Therefore, after the D_2O exchange method all the residual silanols on the modified SBA-15 samples are deuterium exchanged. However, the protons of the alkylsilane moieties are capable of transferring magnetization to the silicon atoms of the residual deuterated silanols. Thus, these shielded deuterated silanols will be detected in the CP NMR

spectrum, even though they can be considered to have limited access to reagents, analytes or large molecules. Therefore, it can be anticipated that if there were changes in the registered ^{29}Si CP NMR spectra before and after deuterium exchange, this would mean that the residual silanol populations would be accessible and non shielded by attached silane molecules.

Insert Figure 6

The CP NMR spectrum of the starting SBA-15 (Fig. 6a) after deuterium exchange shows a remarkable signal decrease. A tentative quantitative analysis reveals that the Q^i site signals are reduced by 87 %. If the original intensity were ascribed to 3.82 OH per nm^{-2} or what is the same, 3.77 $mmol \cdot g^{-1}$, the internal silanols would represent roughly 0.5 $mmol \cdot g^{-1}$. Another interesting feature of this spectrum is that the signal assigned to geminal silanols is not detected after deuterium exchange in SBA-15, what indicates that internal silanols are predominantly of single nature.

The sample TMS-2 (Fig. 6b) after deuterium exchange exhibits a dramatic loss in Q^4 signal. This could indicate the loss of cross polarization source at isolated single silanols which cannot be shielded by vicinal alkylsilane moieties. This hypothesis is supported by the hydrophilic character of the sample.

The sample TMS-3 (Fig. 6c) being intrinsically non-wettable also shows changes in the CP spectrum after deuterium exchange. A deconvolution of the signals by the fitting procedure used in the NMR spectra shows that the changes in the spectra can be due mainly to a decrease in the Q^2 signal. This would mean that the geminal silanols which are sterically hindered to the reaction with an alkylsilane are not cross-polarized by vicinal alkyl chains. It has been reported that a methyl group is only capable of transferring proton magnetization to an average of 0.3 silicon atoms [25].

Therefore, spatially very close deuterated silanols would loose the magnetization. The accessibility of these silanols to larger molecules than D_2O cannot be easily predicted.

Changes in the VTS-TMS spectrum (Fig. 6d) after deuterium exchange are not so obvious. There is a clear diminishing in the T^2 signal intensity which can be ascribed to a further hydrolysis of remaining alkoxy groups with D_2O yielding undetectable OD groups. Concerning the Q region, there is no clear reduction in any of the Q sites, what evidences a successful shielding effect of the attached silane on the residual unreacted silanols. This is consistent with the hypothesis of a crosslinked layer for the organic coverage on the surface of the VTS-TMS sample. Although the number of residual silanols present on the sample is relative high, the accessibility of these to large molecules is very low.

4. Conclusions

An acid-catalyzed post-synthesis method to graft organic groups onto the inner surface of a SBA-15 mesoporous silica has been tested. The yield in the incorporation of mono- and trifunctionals organosilanes was higher and the reaction time shorter than in the conventional toluene reflux strategy. In addition, the grafting reaction proceeded in a controlled manner, remaining the mesoporous character of the material unaffected as deduced by the DRX analysis, TEM and textural properties of the organically modified samples.

The surface nature regarding the number of reacted and unreacted silanols has been thoroughly studied by means of NMR experiments. The quantitative determination of residual silanols in the derivatized samples revealed that the extent of the grafting reaction depends on the silane reagent, being more efficient for small trifunctional molecules, such as vinyltrimethoxy silane. The accessibility of the residual silanols was

qualitatively studied by a deuterium exchange and subsequent ^{29}Si CP NMR experiments. The main conclusion drawn after this latter analysis was that the vinyltrimethoxy silane after an end-capped reaction with trimethyl silane formed a crosslinked layer on the SBA-15 mesoporous surface and the residual silanols were mostly ligand shielded. This surface structure will preclude the access of active molecules to the silanols and then favor the use of these materials in specific applications, such as catalytic processes.

Acknowledgements

We acknowledge financial support from the Spanish Science and Education Ministry (MAT2202-04042-C02-02, 200560M172, CTQ2005-02375). We also thank Carmen Force for NMR solid state measurements. N. García wishes to thank "Programa Ramón y Cajal" for funding. This work has been done in the frame of the EU NoE NANOFUN-POLY.

References

[1] C.T. Kresge, M.E. Leonowicz, W.J. Roth, J.C. Vartulli, J.S. Beck, Nature 359 (1992) 710.

[2] D.Y. Zhao, J.L. Feng, Q.S. Huo, N. Melosh, G.H. Fredrickson, B.F. Chmelka, G.D. Stucky, Science 279 (1998) 548.

[3] D.Y. Zhao, Q.S. Huo, J.L. Feng, B.F. Chmelka, G.D. Stucky, J. Am. Chem. Soc. 120 (1998) 6024.

[4] D. Brunel, Micropor. Mesopor. Mat. 27 (1999) 329.

[5] A. Stein, B. J. Melde, R.C. Schroden, Adv. Mater. 12 (2000) 1403.

[6] J.W. Zhao, F. Gao, Y.L. Fu, W. Jin, P.Y. Yang, D.Y. Zhao, Chem. Commun. 7 (2002) 752.

[7] D.P. Serrano, G. Calleja, J.A. Botas, F.J. Gutierrez, Ind. Eng. Chem. Res. 43 (2004) 7010.

[8] C.M. Crudden, M. Sateesh, R. Lewis, J. Am. Chem. Soc. 127 (2005) 10045.

[9] S.-W. Song, K. Hidajat, S. Kawi, Langmuir 21 (2005) 9568.

[10] S. Perathoner, P. Lanzafame, R. Passalacqua, G. Centi, R. Schloegl, D. S. Su, Micropor. Mesopor. Mat. 90 (2006) 347.

[11] I.G. Shenderovich, G. Buntkowsky, A. Schreiber, E. Gedat, S. Sharif, J. Albrecht, N.S. Golubev, G.H. Findenegg, H.–H. Limbach, J. Phys. Chem. B 107 (2003) 11924.

[12] J.A. Melero, G.D. Stucky, R. van Grieken, G. Morales, J. Mater. Chem. 12 (2002) 1664.

[13] Y. Wang, B. Zibrowius, C.–M. Yang, B. Spliethoff, F. Schüth, Chem. Commun. 1 (2004) 46.

[14] A.S.M. Chong, X.S. Zhao, A.T. Kustedjo, S.Z. Qiao, Micropor. Mesopor. Mat. 72 (2004) 33.

[15] R.A. Garcia, R. van Grieken, J. Iglesias, V. Morales, J. Martin, Stud. Surf. Sci. Catal. 158 (2005) 485.

[16] Sujandi, S.-E. Park, D.-S. Han, S.-C. Han, M.–J. Jin, T. Ohsuna, Chem. Commun. 39 (2006) 4131.

[17] Z. Hua, W. Bu, Y. Lian, H. Chen, L. Li, L. Zhang, C. Li, J. Shi, J. Mater. Chem. 15 (2005) 661.

[18] D.P. Serrano, J. Aguado, R.A. García, C. Vargas, Stud. Surf. Sci. Catal. 158 (2005) 1493.

[19] J.M. Rosenholm, A. Penninkangas, M. Lindén, Chem. Commun 37 (2006) 3909.

[20] R. Palkovits, C.H. Yang, S. Olejnik, F. Schüth, J. Catal. 243 (2006) 93.

[21] E.T. Lippmaa, M.A. Alla, T.J. Pehk, J. Am. Chem. Soc. 100 (1978) 1929; E.T. Lippmaa, M. Maegi, A. Samoson, G. Engelhardt, A.R. Grimmer, J. Am. Chem. Soc. 102 (1980) 4889.

[22] E. Bayer, K. Albert, J. Reiners, M. Nieder, D. Müller, J. Chromatogr. 264 (1983) 197.

[23] D.W.Sindorf, G.E. Maciel, J. Am. Chem. Soc. 103 (1981) 4263; D.W.Sindorf, G.E. Maciel, J. Phys. Chem. 86 (1982) 5208; D.W. Sindorf, G.E. Maciel, J. Am. Chem. Soc. 105 (1983) 3767; I.S. Chuang, D.R. Kinney, G.E. Maciel, J. Am. Chem. Soc. 115 (1993) 8695.

[24] S. Léonardelli, L. Facchini, C. Fretigny, P. Tougne, A.P. Legrand, J. Am. Chem. Soc. 114 (1992) 6412.

[25] A.B. Scholten,; J.W. de Haan, H.A. Claessens, L.J.M. van de Ven, C.A. Cramers, Langmuir 12 (1996) 4741.

[26] K. Albert, J. Sep. Sci. 26 (2003) 215.

[27] A.S.M. Chong, X.S. Zhao, J. Phys. Chem. B 107 (2003) 12650.

[28] W. Hu, Q. Luo, Y. Su, L. Chen, Y. Yue, C. Ye, F. Deng, Micropor. Mesopor. Mat. 92 (2006) 22.

[29] R. Anwander, I. Nagl, M. Windenmeyer, G. Engelhardt, O. Groeger, C. Palm, T. Röser, J. Phys. Chem. B 104 (2000) 3532.

[30] H.-M. Kao, P.-C. Chang, J.-D. Wu, A.S.T. Chiang, C.-H. Lee, Micropor. Mesopor. Mat. 97 (2006) 9.

[31] Q. Tang, Y. Xu, D. Wu, Y. Sun, J. Wang, J. Xu, F. Deng, J. Control. Release 114 (2006) 41.

[32] H. Engelhardt, D. Mathes, J. Chormatogr. 142 (1977) 311.

[33] Y.-H. Liu, H.-P. Lin, C.-Y. Mou, Langmuir 20 (2004) 3231.

[34] G.E. Berendsen, L. de Galan, J. Liq. Chromatogr. 1 (1978) 561.

[35] L.T. Zhuravlev, Colloid. Surface. A 173 (2000) 1.

[36] G. Fóti, E. Kováts, Langmuir 5 (1989) 232.

Figure captions

Figure 1. ^{13}C CP NMR spectra for VTS-w (a), VTS (b), and VTS-TMS (c).

Figure 2. Nitrogen adsorption isotherms and pore size distributions (insert) for the parent SBA-15 and samples modified by grafting.

Figure 3. ^{29}Si CP NMR spectra for SBA-15 (a), VTS-w (b), TMS-3 (c), and VTS-TMS (d).

Figure 4. ^{29}Si NMR spectra for SBA-15 (a), OTS-VTS (b), TMS-2 (c), TMS-3 (d), VTS (e), and VTS-TMS (f).

Figure 5. *Wettability test* for some derivatized samples.

Figure 6. ^{29}Si CP NMR spectra for SBA-15 (a), TMS-2 (b), TMS-3 (c), and VTS-TMS (d), before (top) and after (bottom) deuterium exchange.

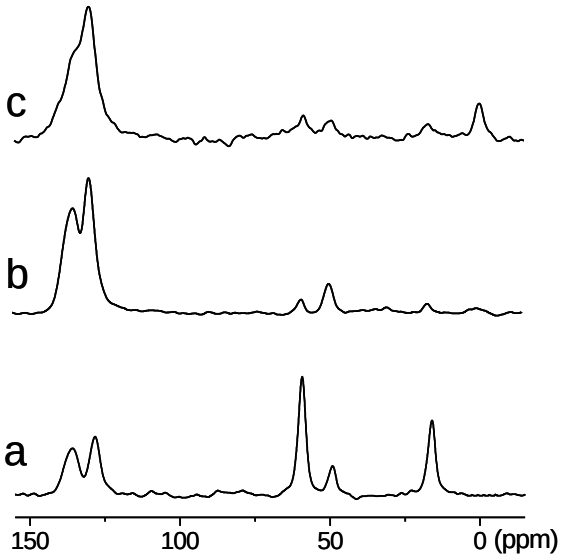

Figure 1: ^{13}C CP/MAS NMR spectra for VTS-w (a), VTS (b), and VTS-TMS (c).

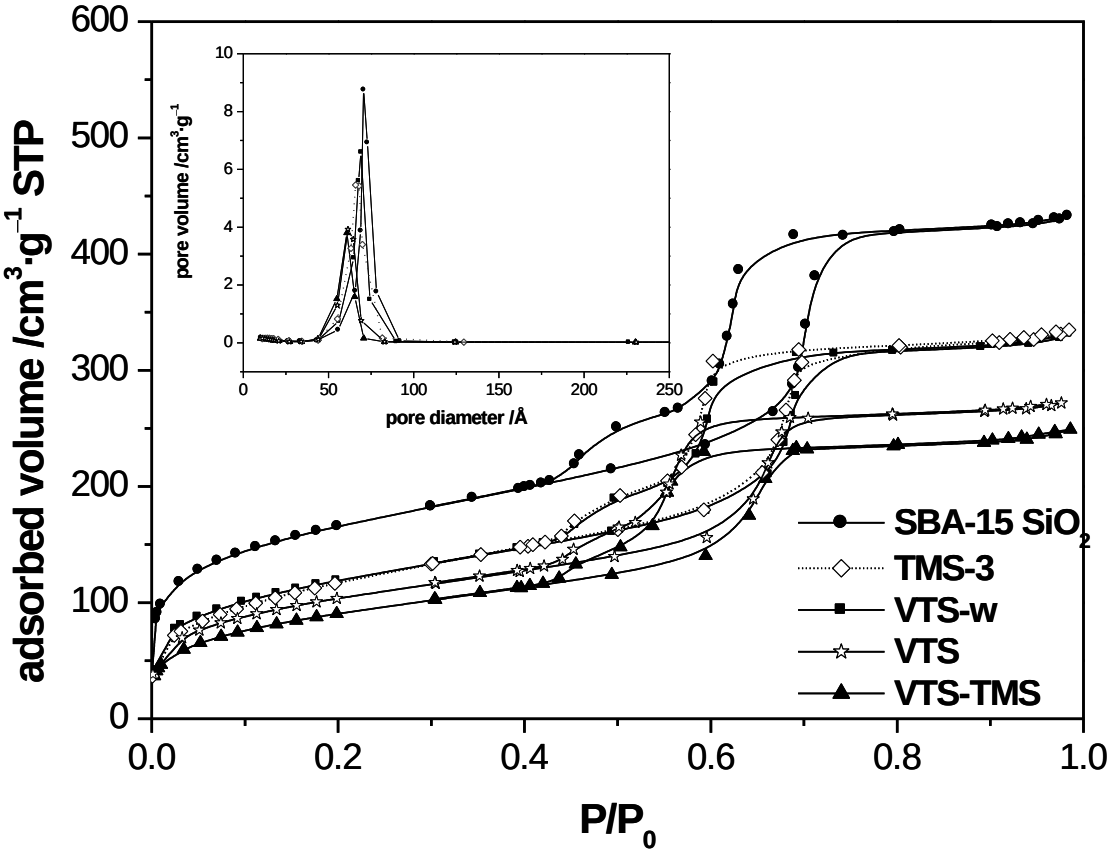

Figure 2. Nitrogen adsorption isotherms and pore size distributions (insert) for the parent SBA-15 and samples modified by grafting.

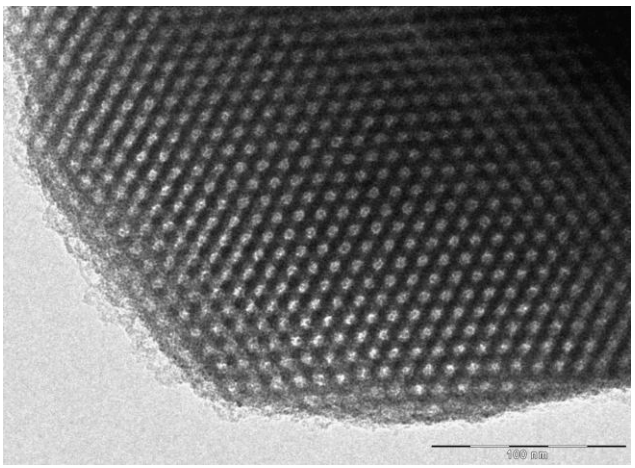

Fig. 3. TEM micrograph of VTS-TMS organically modified sample.

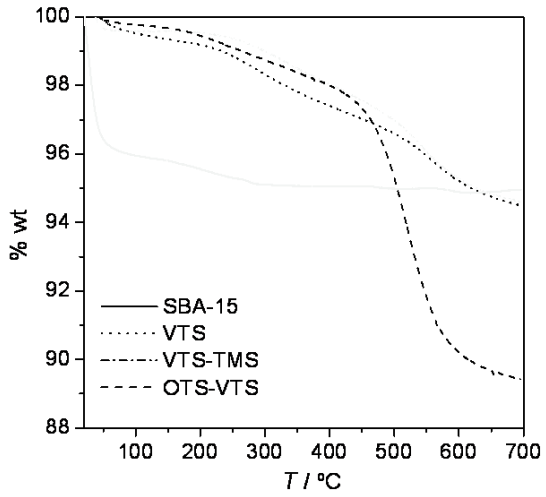

Figure 4: Weight loss in N_2 in dynamic conditions for the starting SBA-15 and some selected derivatized products.

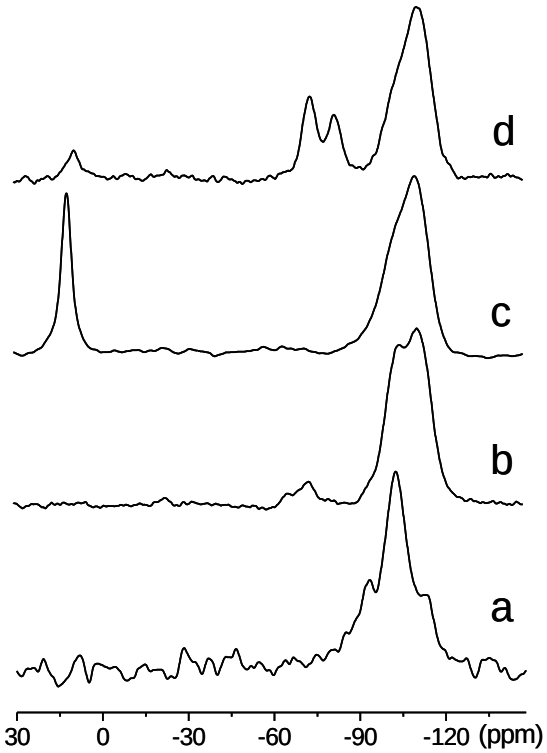

Figure 5: ^{29}Si CP/MAS NMR spectra for SBA-15 (a), VTS-w (b), TMS-3 (c), and VTS-TMS (d).

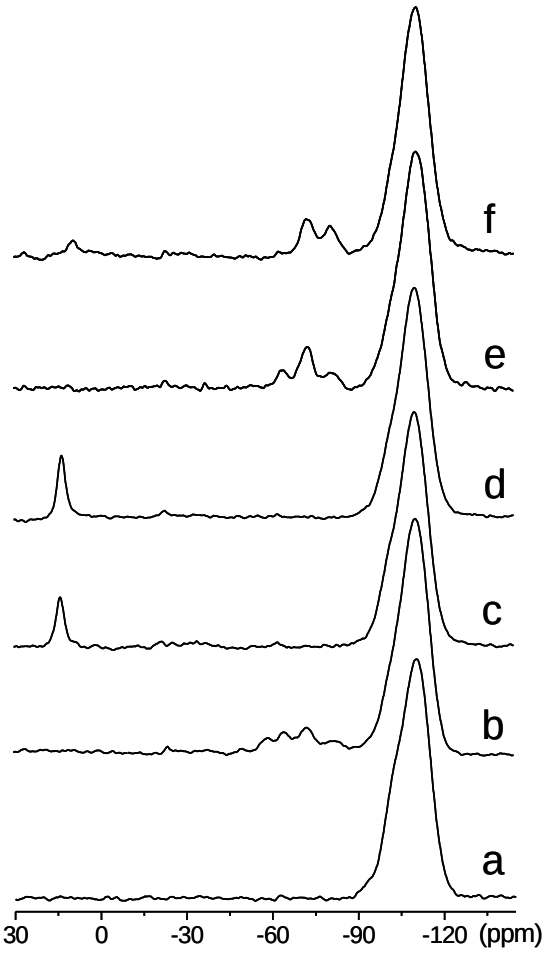

Figure 6: ^{29}Si MAS NMR spectra for SBA-15 (a), OTS-VTS (b), TMS-2 (c), TMS-3 (d), VTS (e), and VTS-TMS (f).

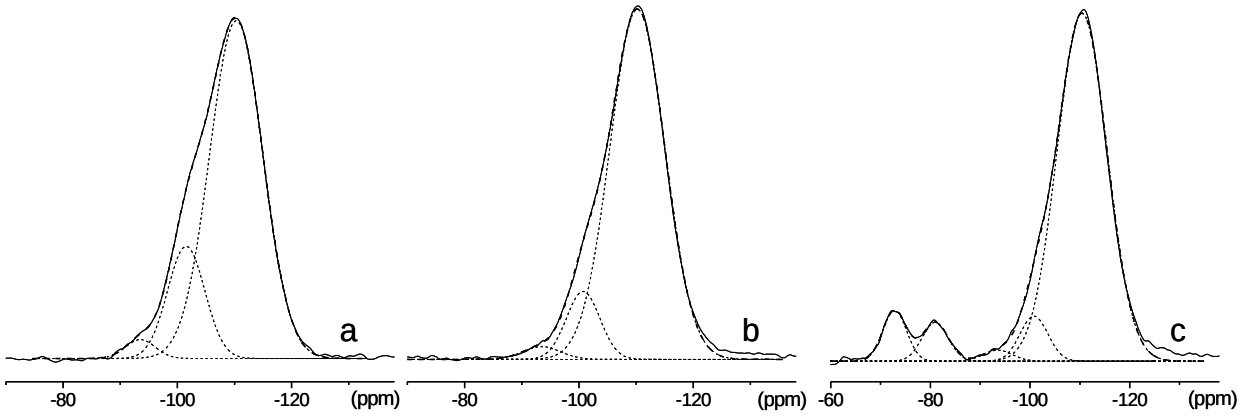

Figure 7: Deconvolutions of selected ^{29}Si MAS NMR spectra from Figure 10: SBA-15 (a), TMS-3 (b), and VTS-TMS (c). The low field region of the spectra where M signal in spectra b and c appears is not shown to better comparison with the SBA-15 spectrum.

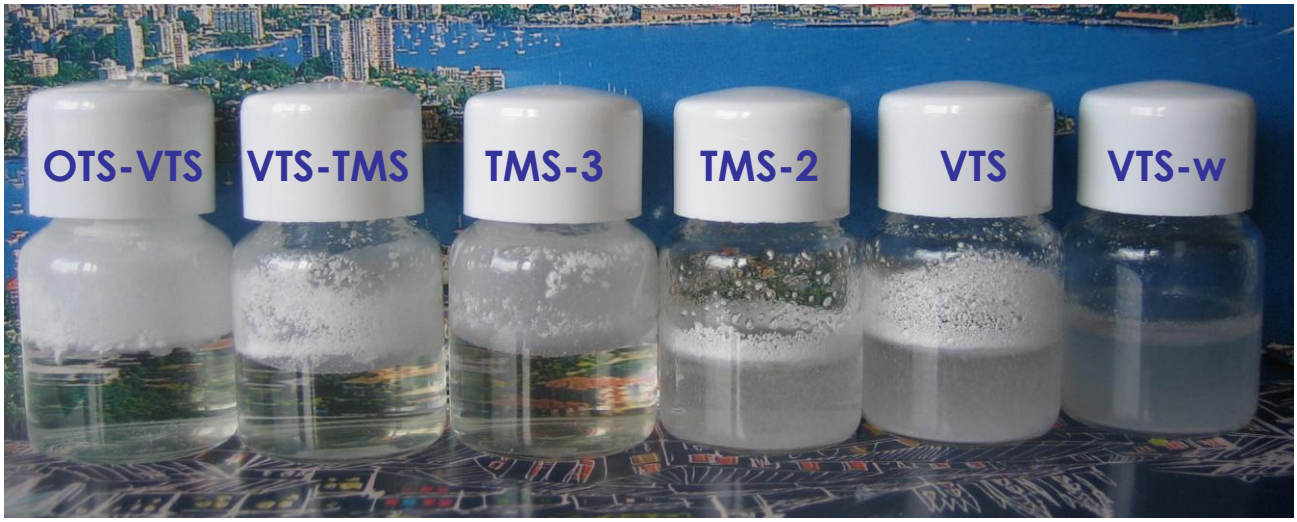

Figure 8. *Wettability test* for some derivatized samples.

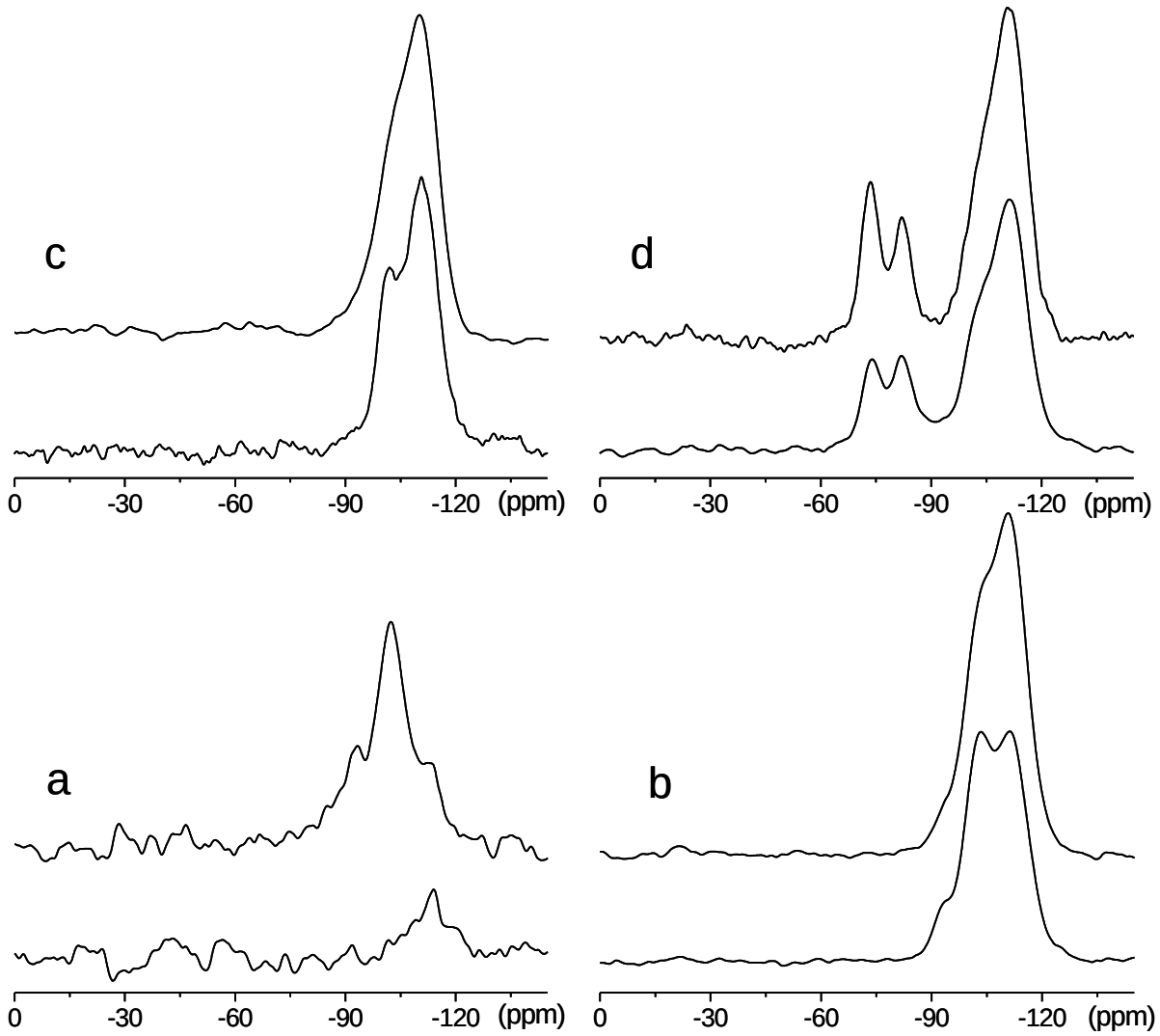

Figure 9. ^{29}Si CP NMR spectra for SBA-15 (a), TMS-2 (b), TMS-3 (c), and VTS-TMS (d), before (top) and after (bottom) deuterium exchange.

Table 1. Summary of the reactions performed and carbon content and textural properties of the resulting derivatized SBA-15 materials.

Sample	**Alkoxysilane**	**%C**	S_{BET} /($m^2 \cdot g^{-1}$)	d_{pore} /(Å)	V /($cm^3 \cdot g^{-1}$	V_{micro} /($cm^3 \cdot g^{-1}$
SBA-15	-	-	593	70.6	0.66	0.17
TMS-1	Trimethylmethoxy	3.34	445	68.8	0.53	0.11
TMS-2	Trimethylmethoxy	3.50	470	69.6	0.55	0.12
TMS-3	Trimethylmethoxy	4.15	433	65.9	0.51	0.11
VTS	Vinyltrimethoxy	5.05	378	61.4	0.42	0.09
VTS-TMS	Trimethylmethoxy	6.18	333	60.8	0.38	0.07
OTS	Octyltrimethoxy	7.26	370	63.3	0.43	0.07
OTS-VTS	Vinyltrimethoxy	9.37	297	53.9	0.34	0.06
VTS-w	Vinyltrimethoxy	3.37	433	69.1	0.51	0.11

Table 2: Molar weight, MW, molar fractions of Q^i sites, w Q^i, total number of residual unreacted silanols, OH_{res}, and calculated carbon content, $\%C_{cal}$, for the starting SBA-15 and some derivatized samples. The numbers in brackets correspond to the relative peak areas (%) for the Q^i species.

Sample	**MW /(g·mol^{-1})**	**wQ^{2*}**	**wQ^{3*}**	**wQ^{4*}**	**OH_{res} /(nm^{-2})**	**$\%C_{cal}$**
SBA-15	62.11	0.025(2.5)	0.184(18.4)	0.791(79.1)	3.83	-
TMS-2	62.12	0.019(2.0)	0.123(13.0)	0.802(84.9)	2.63	3.2
TMS-3	62.08	0.020(2.1)	0.096(10.3)	0.813(87.5)	2.22	4.1
VTS	64.56	0.013(1.5)	0.083(9.4)	0.784(89.0)	1.71	5.2
VTS-TMS	63.33	0.015(1.7)	0.058(6.6)	0.806(91.7)	1.41	6.0
OTS-VTS	69.68	0.022(2.5)	0.110(12.6)	0.74(84.9)	2.25	11.1

*The numbers in brackets correspond to the relative peak areas (%) for the Q^i species.

Table 3: Initial number of surface silanols, OH_i, number of attached silane silicons, Γ, global extent of the surface reaction, θ, and relative reaction of geminal, θ_g, and single, θ_l, silanols calculated for some derivatized samples.

Sample	OH_i /(nm^{-2})	Γ /(nm^{-2})	θ	θ_g	θ_l
TMS-2	4.12	1.06	0.28	0.14	0.30
TMS-3	3.99	1.28	0.38	0.11	0.42
VTS	3.08	1.62	0.59	0.49	0.60
VTS-TMS	3.33	1.95	0.65	0.34	0.69